Acta Crystallographica Section B
Structural Science
ISSN 0108-7681

Disordered crystal structure of pentamethylcyclopentadienylsodium as seen by high-resolution X-ray powder diffraction

Consiglia Tedesco,[a] Robert E. Dinnebier,[b]*† Falk Olbrich[c] and Sander van Smaalen[b]

[a]Dipartimento di Chimica, Università di Salerno, via S. Allende, I-84081 Baronissi, Italy, [b]Lehrstuhl für Kristallographie, Universität Bayreuth, D-95440 Bayreuth, Germany, and [c]Institut für Anorganische Chemie, Universität Hamburg, D-20146 Hamburg, Germany

† Present address: Max Plank Institute for Solid State Research, Heisenbergstrasse 1, D-70569 Stuttgart, Germany.

Correspondence e-mail: r.dinnebier@fkf.mpg.de

Received 1 June 2001
Accepted 21 July 2001

The crystal structure of pentamethylcyclopentadienylsodium, $[NaC_{10}H_{15}]$ (NaCp*), has been determined from high-resolution X-ray powder diffraction. The compound crystallizes in space group *Cmcm* with lattice parameters $a = 4.61030\ (3)$, $b = 16.4621\ (3)$, $c = 14.6751\ (2)$ Å, $V = 1113.77\ (4)$ Å^3 ($Z = 4$). NaCp* forms polymeric multidecker chains along the *a* axis. The Rietveld refinement ($R_p = 0.050$ and $R_F = 0.163$) shows that the Cp* moieties occupy, with disorder, two different orientations rotated away from the eclipsed conformation by $\pm 13.8^\circ$.

Dedicated to Professor Guido Sodano, Professor of Organic Chemistry, University of Salerno. His example as a scientist and teacher lives beyond his death.

1. Introduction

Organometallic compounds with alkali elements are common reactants or intermediates in organic synthesis. In particular, the alkali metal salts of pentamethylcyclopentadiene are important reagents for attaching pentamethylcyclopentadienyl (Cp*) groups to metal complexes. This ligand has played a significant role in organic chemistry during the past decades, due to both steric and electronic influences imparted by the methyl substituents on the corresponding metal compounds (Jutzi, 1987). Cp* complexes are generally much more stable than the corresponding cyclopentadienyl species due to kinetic and thermodynamic effects. Moreover, the presence of Cp* ligands enhances the solubility of transition metal complexes in organic solvents.

In recent years there has been a growing interest in the solid-state structures of alkali metal cyclopentadiene derivatives. Up to a few years ago a relatively small number of stable crystalline alkali metal salts of cyclopentadiene derivatives have been isolated and their structures have been determined. They mainly consisted of solvated adducts (Weiss, 1993). This can be understood considering the poor solubility and sensitivity for oxidation of this kind of compound, which makes it almost impossible to grow single crystals suitable for X-ray diffraction analysis.

Recently, the advances in X-ray powder diffraction methods allowed the structure determination of several solvent-free organoalkali compounds LiCp, NaCp, KCp (Dinnebier, Behrens & Olbrich, 1997); RbCp (Dinnebier, Olbrich, van Smaalen & Stephens, 1997); CsCp (Dinnebier, Olbrich &

© 2001 International Union of Crystallography
Printed in Great Britain – all rights reserved

Bendele, 1997); PhLi (Dinnebier *et al.*, 1998); LiCp* (Dinnebier, Schneider *et al.*, 1999); indenyllithium and fluorenylsodium (Dinnebier, Neander *et al.*, 1999).

In this report the structure solution and refinement of the pentamethylcyclopentadienylsodium (NaCp*) from high-resolution X-ray powder diffraction data will be discussed and the structure will be compared with that of the structurally related compounds: cyclopentadienylsodium (NaCp) and pentamethylcyclopentadienyllithium (LiCp*).

In the case of metallocene compounds the accurate structure determination is often complicated by the presence of disorder; $FeCp_2$ (Seiler & Dunitz, 1979, 1982) and $CaCp_2$ (Zerger & Stucky, 1974) are common examples. In fact, the rotation of the rings about an axis perpedicular to the planes of the rings show a very low energy barrier (Dinnebier, Schneider *et al.*, 1999; Braga, 1992). Thus, it is not unusual to find rotational disorder in the crystalline structures of metallocene compounds. Recently it has been shown that LiCp* exhibits threefold rotational disorder of the Cp* moieties. Presently a disordered structure is also found for NaCp*, as it is also indicated by the rapid decrease of the intensities with increasing scattering angles (Fig. 1). Different types of disorder have been modelled by Rietveld refinement (Rietveld, 1969) from high-resolution X-ray powder diffraction data.

2. Experimental

NaCp* was prepared according to the literature (den Haan *et al.*, 1986; Rabe *et al.*, 1991). Freshly distilled HC_5Me_5 and carefully washed (cyclopentane) NaH were stirred in tetrahydrofuran under reflux for 5 d. The mixture was placed into a Soxhlet apparatus, extracted for 1 d, filtered and the solvent removed under reduced pressure until a solid started to precipitate. The white product was washed with cyclopentane and dried in vacuum.

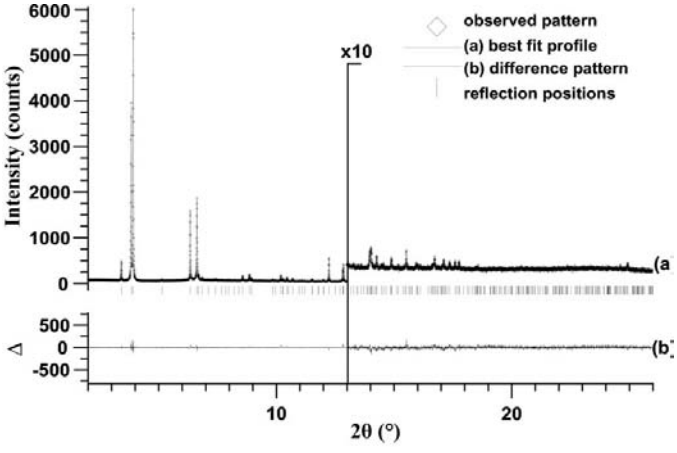

Figure 1
Scattered intensity of NaCp* at $T = 295$ K as a function of the diffraction angle 2θ. Shown are the observed pattern (◇), the best fit profile in *Cmcm* (a), the difference curve between observed and calculated profiles (b) and the reflection markers (vertical bars). The wavelength is λ = 0.491213 (2) Å. The higher-angle part starting at 13° 2θ is enlarged by a factor of 10.

Lithiumborate glass (Hilgenberg, glass No. 50, 0.7 mm) capillaries were filled with the air-sensitive powder of NaCp* and sealed with piceine in a dry-box under argon atmosphere.

X-ray powder diffraction data of NaCp* were collected on the high-resolution powder diffractometer at the beamline BM16 of the European Synchrotron Radiation Facility (ESRF). The diffraction pattern is shown in Fig. 1. The X-rays from the bending magnet source were collimated vertically by a rhodium-coated silicon mirror before they are incident on the double crystal monochromator. A Si(111) reflection was used to select an X-ray energy of 24 keV. The size of the beam was adjusted to 2×0.6 mm^2 using slits. The wavelength was determined to 0.491213 (2) Å from a silicon standard. The samples were spun during measurements in order to improve randomization of the crystallites. The diffracted beam was analyzed with a nine crystal analyzer stage [nine Ge(111) crystals separated by 2° intervals] and detected with nine Na(Tl)I scintillation counters simultaneously. The incoming beam was monitored by an ion-chamber for normalization for the decay of the primary beam. In this parallel beam configuration, the resolution is determined by the analyzer crystal rather than by slits (Cox, 1991). Details of the experimental setup are described in the beamline handbook (Fitch, 1996). Data were taken at room temperature in continuous scanning mode for several hours and they were normalized against monitor counts and detector efficiency and converted to step scan data in steps of 0.003° 2θ. Low-angle diffraction peaks displayed a FWHM of 0.011° 2θ at room temperature, significantly broader than the resolution of the spectrometer which is estimated to be as low as 0.002 °2θ for the selected wavelength. Experimental details are given in Table 1.[1]

Data reduction was performed using the program *GUFI* (Dinnebier & Finger, 1998). Indexing with *ITO* (Visser, 1969) led to a C-centred orthorhombic cell with four molecules in the unit cell. The observed systematic absences account for two possible space groups, $Cmc2_1$ and *Cmcm*. The peak profiles and precise lattice parameters were determined by LeBail-type fits using the program *GSAS* (LeBail *et al.*, 1988; Larson & Von Dreele, 1994). The background was modelled manually using *GUFI*. The peak profile was described by a pseudo-Voigt function, in combination with a special function that accounts for the asymmetry due to axial divergence (Thompson *et al.*, 1987; Finger *et al.*, 1994). No absorption correction was applied to the data considering the low absorption coefficient and the low packing density.

To account for the strong anisotropy in the half width of the reflections, we used the model by Stephens (1999), which has recently been implemented in profile function No. 4 in the Rietveld refinement program *GSAS* (Larson & Von Dreele, 1994). Refinement of this model was performed stepwise. Initially only the S_{400}, S_{040} and S_{004} coefficients were refined.

[1] Supplementary data for this paper are available from the IUCr electronic archives (Reference: NA0125). Services for accessing these data are described at the back of the journal.

Table 1
Crystallographic data for the room-temperature phase of NaCp*.

R_p and R_{wp} refer to the Rietveld criteria of fit for profile and weighted profile, respectively, defined by Langford & Louër (1996).

Formula	$NaC_{10}H_{15}$
Formula weight (g mol^{-1})	158.22
μ (cm^{-1})	0.195
Packing density (%)	60
Wavelength (Å)	0.491213 (2)
Step size (° 2θ)	0.003 (after rebinning)
Z	4
a (Å)	4.61030 (3)
b (Å)	16.4621 (3)
c (Å)	14.6751 (2)
V (Å^3)	1113.77 (4)
D_{calc} (g cm^{-3})	0.943
Space group	*Cmcm*
R_p LeBail	4.3
R_{wp} LeBail	5.6
Temperature (K)	295

Table 2
Refined profile and strain parameters corresponding to profile function No. 4 in the Rietveld refinement program *GSAS* (Larson & Von Dreele, 1994).

$U = V = W$	0
P	0.0
X	0.072 (1)
ζ	1.0
S_{400}	0.052 (4)
S_{040}	0.0015 (2)
S_{004}	0.0032 (2)
S_{220}	0.041 (3)
S_{202}	0.224 (6)
S_{022}	0.0035 (3)
S/L	0.00547 (2)
H/L	0.004

After convergence the S_{220}, S_{202} and S_{022} terms were added and finally the mixing coefficient between the Gaussian and the Lorentzian fraction of the peak width, ζ, was added to the refinement. The refined profile parameters including the refined anisotropic strain-broadening values S_{HKL} are given in Table 2. The refined profile is purely Lorentzian with a small L_x value, from which the size P of the presumably spherical grains may be estimated to be 3.5 µm according to $P(\mu m) = (180/\pi)(0.9\lambda/L_x 100)$. A graphical visualization of the three-dimensional microstrain distribution of NaCp* using the refined S_{HKL} values is given in Fig. 2, from which it can be seen that the strain is small along the main crystallographic axes and maximum along the bisector between a and c axes. It may be assumed that the internal strain is mainly caused by interaction of the disordered bulky Cp* rings of neighbour chains, where the Cp* rings are facing each other directly. Therefore, a small strain along the crystallographic a axis can be understood, since the individual chains are presumably strain free with small variations in distance between the Cp* ring and the Na atoms. Along the b direction, the Cp* molecules do not face each other directly and along the c direction, the distances between neighbouring chains are quite large.

Low-temperature scans have been performed at the high-resolution X-ray powder beamline X3B1 of the National Synchrotron Light Source at Brookhaven National Laboratory. NaCp* was cooled down to 25 K in a closed-cycle helium cryostat. As for LiCp* (Dinnebier, Schneider *et al.*, 1999), a phase transition was observed at ~190 K, indicated by the onset of a broadening of the diffraction maxima. This phase transition was found to be reversible because the diffraction maxima sharpen again when heating the sample up to room temperature. A complete scan was taken at 25 K using a wavelength of 1.15031 (1) Å for 10.2 s at each 2θ in steps of 0.015 from 5 to 35.0° and for 12.2 s at each 2θ from 35.0 to 48.6° (see Fig. 3). Although an ω scan did not reveal severe grain size effects, the sample was rocked by 20° during measurement. The evidently low symmetric pattern of the low-temperature phase could not be indexed unambiguously. In addition, LeBail fits of several superstructures with monoclinic and orthorhombic symmetries based on the unit cell at room temperature have been tried. None gave a satis-

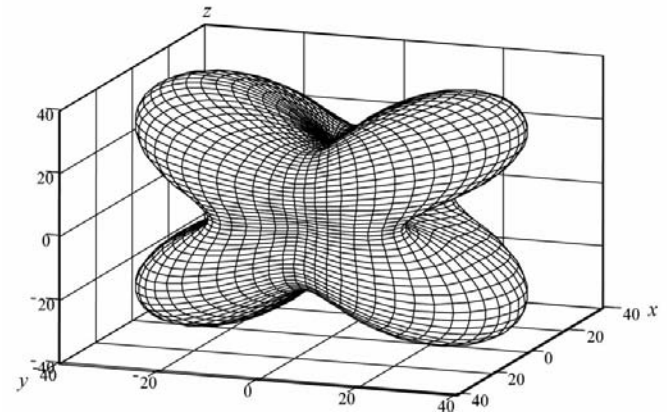

Figure 2
Perspective view of the three-dimensional strain distribution of NaCp*. The x axis is horizontal, z axis vertical and the y axis out of the paper. The scale is in $\delta d/d * 10^{-6}$ strain.

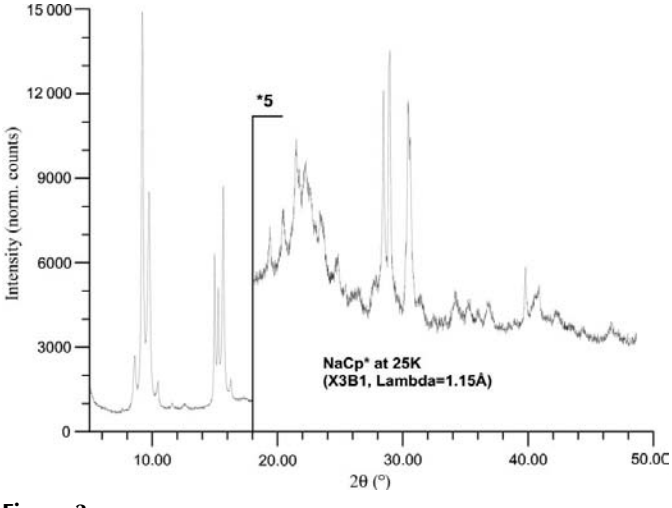

Figure 3
Scattered intensity of NaCp* at T = 25 K as a function of the diffraction angle 2θ. The wavelength is λ = 1.15031 (2) Å. The higher angle part starting at 18.0° 2θ is enlarged by a factor of 5.

Table 3
Refinement results for the different disorder models of NaCp* in *Cmcm* and $Cmc2_1$ space groups.

The best model according to the criteria as described in the text is highlighted in bold.

Disorder type	φ_a (°)	No. of parameters	Space group	R_p	R_{wp}	R_F	R_{F^2}
None	0	8	*Cmcm*	0.063	0.099	0.198	0.202
None	–9.7 (1)	11	$Cmc2_1$	0.058	0.067	0.170	0.156
Twofold	0, 36	8	*Cmcm*	0.052	0.072	0.172	0.148
Twofold	13.89 (9)	**9**	*Cmcm*	**0.050**	**0.066**	**0.163**	**0.136**
Twofold	20.1 (3), −6.8 (5)	12	$Cmc2_1$	0.050	0.065	0.157	0.133
Threefold	0, 24	8	*Cmcm*	0.052	0.071	0.165	0.142
Threefold	0, 17.9 (1)	9	*Cmcm*	0.050	0.066	0.159	0.138
Threefold	0, 21.4 (5)	10	*Cmcm*	0.050	0.066	0.157	0.136

factory fit. This failure is attributed to the partially extreme line broadening with many closely overlapping reflections. It is very likely that there is at least partial order of the Cp* molecules at low temperatures, which often results in very low symmetry as in the case of triclinic $FeCp_2$ below 148 K (Calvarin & Berar, 1975).

3. Structure solution and Rietveld refinements

The starting point for the structure solution was the observation that the length of the *a* axis of NaCp* [4.61030 (3) Å] is similar to that of the *c* axis of NaCp [4.7128 (2) Å]. This latter compound shows a multidecker structure in the direction of the *c* axis, thus a similar structure can also be inferred for NaCp*. Moreover, the *c* axis of NaCp* [14.6751 (2) Å] is similar to the *a* axis of the analogous compound LiCp* [14.7711 (5) Å], and the ratio between the *c* and *b* axes in NaCp* is only 2.9% greater than $3^{1/2}/2$, thus suggesting the possibility that the orthorhombic lattice produced by NaCp* could be seen as a distortion of the rhomboedral lattice of LiCp*. Therefore, the positions of the centroid of the cyclopentadienyl ring and the Na atom could be roughly estimated from the beginning.

In the subsequent Rietveld refinement procedures all profile and lattice parameters were fixed to the values obtained by the LeBail fit and only the structural parameters were allowed to vary. In order to reduce the number of variables to be refined, the cyclopentadienyl ring was described as a regular pentagon with fixed C—C bond lengths (1.42 Å for the C—C bond lengths of the inner ring and 1.50 Å for the C—CH_3 bond lengths). Rigid-body refinements were performed in both space groups $Cmc2_1$ and *Cmcm*, considering as variables the coordinates of the Na atom, the translational and rotational parameters of the rigid body and atomic displacement parameters. The displacement parameters of the Na atom were refined anisotropically, while the isotropic displacement parameters for the C atoms of the inner ring and for the methyl groups were allowed to refine independently. The fractional occupancy of each methyl C atom was assumed to be 1.5 times that of the C atoms in the cyclopentadienyl ring, in order to account for the electron density of the entire CH_3 group (presumably disordered), which accounts for nine electrons *versus* six for a single C atom. In fact, although the positions of the H atoms cannot usually be determined experimentally by X-ray powder diffraction, their contribution to the profile is definitely measurable (Dinnebier, Schneider *et al.*, 1999; Lightfoot *et al.*, 1993).

At first ordered models were considered in both space groups *Cmcm* and $Cmc2_1$. According to the symmetry restrictions for the ordered models, the Cp* ring in *Cmcm* has only one translational degree of freedom along the *b* axis (τ_b), while in $Cmc2_1$ also the rotation ϕ_a about an axis passing through the center of gravity of the ring, perpendicular to the molecular plane and parallel to the crystallographic *a* axis, must be considered. None of these models

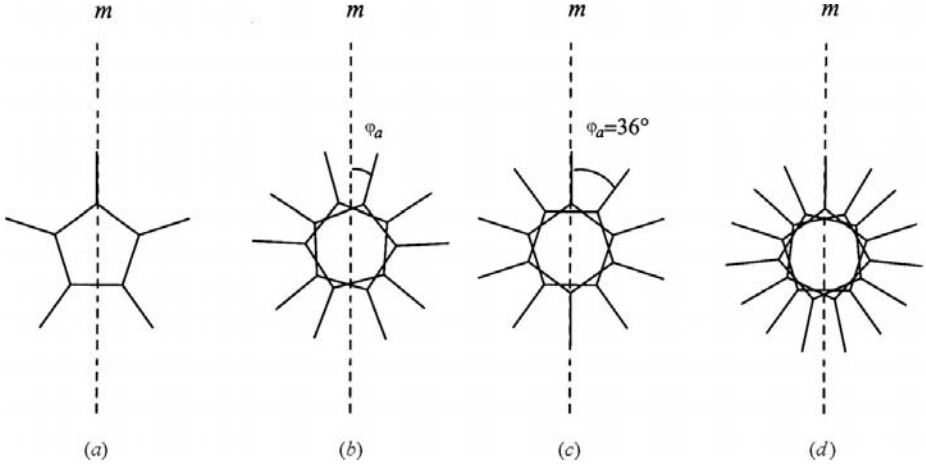

Figure 4
(*a*) Ordered model, (*b*), (*c*) twofold and (*d*) threefold disordered models in *Cmcm*. The mirror plane through the ring centroid is shown as the dashed line.

gave a completely satisfactory fit to the data, suggesting the presence of disorder as was found for LiCp*.

Secondly, structure models with different types of rotational disorder were considered, including twofold and threefold disorder of the Cp* in both space groups. The results of the various refinement are compared in Table 3.

A twofold disorder model in *Cmcm* can be derived directly from the *Cmcm* ordered model, allowing the ϕ_a rotation angle to be different from 0° and refinable; in fact, the mirror plane will produce a second Cp* ring superimposed on the previous one for any value different from a multiple of 36°, see Fig. 4(*b*).

A twofold disorder model can also be built in *Cmcm* defining two rigid Cp* rings superimposed on each other, with the same τ_b translational parameters, but φ_a values fixed at 0 and 36°, respectively, see Fig. 4(*c*). The same also applies to the space group $Cmc2_1$, but in this case both φ_a rotation angles of the two superimposed Cp* moieties are allowed to be refined individually.

A threefold disorder model can be built in *Cmcm* by the superposition of a Cp* molecule with $\varphi_a = 0°$ and a pair of Cp* moieties at $\pm\varphi_a \neq 0°$. For $\varphi_a = \pm 24°$ the three moieties are equally distributed on a ring and this model resembles the disorder as was found for rhombohedral LiCp*. However, within the orthorhombic symmetry the parameter φ_a is allowed to vary freely, see Fig. 4(*d*). Accordingly, three different refinements for a threefold disorder model were performed in *Cmcm*:

(i) fixing the value of the φ_a rotation angle of the second rigid body to 24° (8 parameters);

(ii) allowing it to be refined (9 parameters);

(iii) also refining a constrained occupancy factor for the atoms of the three Cp* rings (10 parameters).

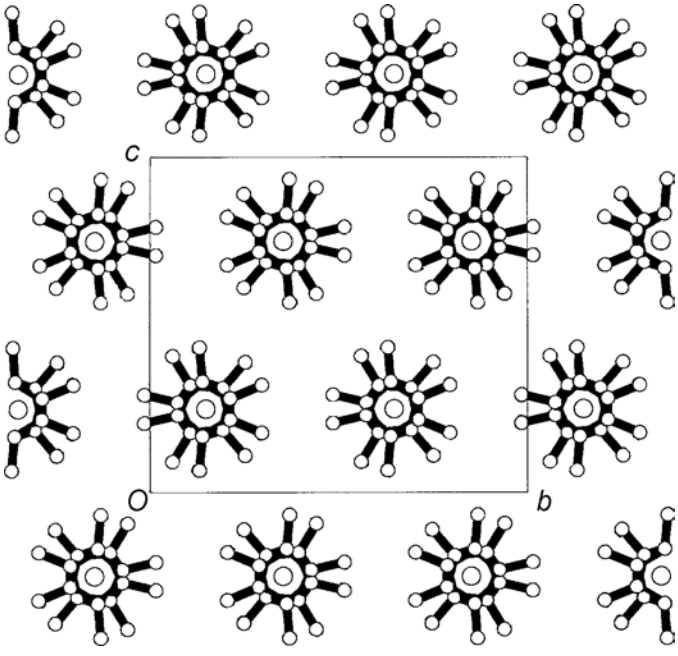

Figure 5
Packing for the twofold disordered model in *Cmcm*; view along the *a* axis.

In order to build a threefold disorder model in $Cmc2_1$, three rigid Cp* rings superimposed onto each other must be defined; the τ_b translation will be the same for both three rings and the φ_a rotation angles will be allowed to vary independently. Any attempt to refine a threefold model in the space group $Cmc2_1$ failed due to divergence of the refinement.

It seems that the disordered structure of NaCp* can be described by the twofold disorder model in *Cmcm*, where a Cp* ring is crossed by two mirror planes perpendicular to each other and the other is rotated by 13.89 (9)° with respect to the first. Criteria for the selection of this model included the fact that it was the simplest model with the lowest *R* values in R_{F^2} and R_{wp} (Table 3).

The refinement of the Cp* atom occupancy factors in the *Cmcm* threefold disorder model led to higher occupancy values for C atoms belonging to the ring with φ_a fixed at 0 than those belonging to the other two rings with $\varphi_a \neq 24°$. This could also indicate that a twofold disorder model is to be preferred. A similar type of disorder was found in the room-temperature crystal structure of ferrocene (Seiler & Dunitz, 1979; Takusagawa & Koetzle, 1979) with a value of the rotation angle of ∼12° from the eclipsed position.

Atomic fractional coordinates, fractional occupancies and displacement parameters for the twofold disorder model have been deposited. The anisotropic displacement parameters of the sodium atom show that the displacement ellipsoid is oblate along the *a* axis. The same result was obtained for NaCp (Dinnebier, Behrens & Olbrich, 1997) and can be understood considering that the chain structure has a lower flexibility in the direction of the chain than in the *bc* plane.

4. Discussion

The structure of NaCp* consists of chains of alternating Na atoms and Cp* rings parallel to the *a* axis (Fig. 5). Similar types of multidecker structure were found for the structures of the related compounds NaCp, LiCp and LiCp*.

Each cyclopentadienyl ring is η^5-coordinated to two Na atoms. The Na—C bond lengths range between 2.579 (2) and 2.624 (2) Å, similar to those found in NaCp [2.631 (12)–2.671 (6) Å] and in anionic sodocene compounds [2.584 (3)–2.670 (3) Å]: $[Ph_4P]^+[Cp_2Na]^-$ (Harder *et al.*, 1996) and $[(TAS)_2Cp]^+[Cp_2Na]^-$, TAS = $(Me_2N)_3S^+$ (Wessel *et al.*, 1995). Slightly longer distances were found by Rabe *et al.* (1991) in the compound NaCp*·3pyridine [2.658 (5)–2.701 (5) Å], while definitely longer Na—C bond lengths were observed by Aoyagi *et al.* (1979) in the polymeric zigzag chain of the compound $[NaCp(TMEDA)]_n$ [2.829 (14)–3.033 (12) Å] (TMEDA = tetramethylethylenediamine). These observations are consistent with the fact that Cp* or Cp groups in solvent-free compounds experience a greater electron withdrawal from the central Na atom.

It is interesting to compare the values of the chain axes (*i.e.* the values of the lattice parameter along which the chain is running) in cyclopentadienyl and pentamethylcyclopentadienyl compounds: LiCp 3.9366 (1) Å and LiCp*

3.82206 (6) Å, NaCp 4.7128 (2) Å and NaCp* 4.61030 (3) Å. Pentamethylcyclopentadienyl compounds show the shortest values of the chain axes.

The distance between the Na atom and the centroid of the Cp* ring is 2.3057 (1) Å, slightly shorter than for NaCp, 2.357 (1) Å. As shown by the fact that the Na—C bond lengths are slighltly different, the coordination of the cyclopentadienyl rings to the Na atom is not exactly symmetric: a line between the centroid of the rings and the metal atom is slightly bent [the angle $Cp_{cent}—Na—Cp_{cent}$ is 177.3 (2)°]. The same feature was observed in NaCp (177.7°) and LiCp (176.4°), but not in LiCp* (180°). We believe that this could be ascribed to interchain interactions.

The crystal packing for the best model in *Cmcm* is shown in Fig. 5. Each chain is surrounded by six other chains forming a distorted hexagon, four are shifted by half the *a* axis, two have the same height. Each Cp* ring is surrounded by four Na atoms and two Cp* rings lying in the same plane. The same arrangement was found in LiCp and NaCp compounds which crystallize in space group *Pnam*. Also LiCp* shows a hexagonal packing of the chains, but all six neighbouring chains are shifted alternatively by either +1/3 or −1/3 of the chain repeat distance. Each Cp* ring is surrounded by six Li atoms at ±1/6 of the chain repeat. Therefore, it could be inferred that the $Cp_{cent}—M—Cp_{cent}$ angle is not determined by interactions between consecutive molecules in the same chain, rather it depends mainly on the nature and strength of the interactions between the metal atom of one chain and C atoms of neighbouring chains. Intramolecular distances between the centroid of the ring and the four coplanar Na atoms range from 8.129 (2) to 8.283 (4) Å, while the distances between the centroids of the two neighbouring chains at the same height are both equal to 8.760 (1) Å. Intramolecular chain contacts involve only the C atoms of the methyl groups: the shortest C···C contact [3.343 (3) Å] involves two methyl groups of Cp* rings at the same height with opposite orientation with respect to the eclipsed position. Other packing distances are equal or greater than 3.872 Å.

5. Conclusions

We have determined the crystal structure of NaCp* by Rietveld refinements against powder diffraction data. The structure is found to be built of NaCp* polymeric chains, as found in other alkali metallocene compounds. The Cp* moieties are found to occupy, with disorder, two orientations which are related by a rotation about the chain axis. This has been compared with the fully ordered structures of NaCp and LiCp, and with the structure of LiCp*, which shows threefold disorder of the Cp* unit. The different space groups of these compounds reflect the different distortions of the structure from an idealized hexagonal arrangement of infinite cylindrical columns.

We are grateful to Andy Fitch (BM16, ESRF) and Peter Stephens (X3B1, NSLS) for their assistance during the measurements. Diffraction measurements at ESRF were carried out under the general user proposal CH-846. Research was carried out in part at the National Synchrotron Light Source at Brookhaven National Laboratory, which is supported by the US Department of Energy, Division of Materials Sciences and Division of Chemical Sciences. The SUNY X3 beamline at NSLS is supported by the Division of Basic Energy Sciences of the US Department of Energy under Grant No. DE-FG02-86ER45231. Financial support by the Deutsche Forschungsgemeinschaft (DFG), the Fonds der Chemischen Industrie, the Italian Ministero dell'Università e della Ricerca Scientifica e Tecnologica (MURST) and the Italian Consiglio Nazionale delle Ricerche (CNR) is gratefully aknowledged.

References

Aoyagi, T., Shearer, H. M. M., Wade, K. & Whitehead, G. (1979). *J. Organomet. Chem.* **175**, 21–31.
Braga, D. (1992). *Chem. Rev.* **92**, 633–665.
Calvarin, G. & Berar, J. F. (1975). *J. Appl. Cryst.* **8**, 380–385.
Cox, D. E (1991). *Handbook of Synchrotron Radiation*, edited by G. Brown and D. E. Moncton, Vol. 3, ch. 5. Amsterdam: Elsevier.
Dinnebier, R. E., Behrens, U. & Olbrich, F. (1997). *Organometallics*, **16**, 3855–3858.
Dinnebier, R. E., Behrens, U. & Olbrich, F. (1998). *J. Am. Chem. Soc.* **120**, 1430–1433.
Dinnebier, R. E. & Finger, L. (1998). *Z. Kristallogr. Suppl.* **15**, 148; available at http://www.pulverdiffraktometrie.de.
Dinnebier, R. E., Neander, S., Behrens, U. & Olbrich, F. (1999). *Organometallics*, **18**, 2915–2918.
Dinnebier, R. E., Olbrich, F. & Bendele, G. M. (1997). *Acta Cryst.* C**53**, 699–701.
Dinnebier, R. E., Olbrich, F., van Smaalen, S. & Stephens, P. W. (1997). *Acta Cryst.* B**53**, 153–158.
Dinnebier, R. E., Schneider, M., van Smaalen, S., Olbrich, F. & Behrens, U. (1999). *Acta Cryst.* B**55**, 35–44.
Finger, L. W., Cox, D. E. & Jephcoat, A. P. (1994). *J. Appl. Cryst.* **27**, 892–900.
Fitch, A. N. (1996). *Mater. Sci Forum*, **228–231**, 219–231; in European Powder Diffraction Conference, EPDIC IV, edited by R. J. Cernick, Delhez, R. & Mittemeijer, R.; http://www.esrf.fr/exp_facilities/BM16/handbook/handbook.html.
Haan, K. H. den, de Boer, J. L., Teuben, J. H., Spek, A. L., Kojic Prodic, B., Hays, G. R. & Huis, R. (1986). *Organometallics*, **5**, 1726–1733.
Harder, S., Prosenc, M. H. & Rief, U. (1996). *Organometallics*, **15**, 118–122.
Jutzi, P. (1987). *Commun. Inorg. Chem.* **6**, 123–144.
Langford, J. I. & Louër, D. (1996). *Rep. Prog. Phys.* **59**, 131–234.
Larson, A. C. & Von Dreele, R. B. (1994). *GSAS*. LANL Report LAUR 86–748. Los Alamos National Laboratory, Los Alamos, USA. Available by anonymous ftp from mist.lansce.lanl.gov.
LeBail, A., Duroy, H. & Fourquet, J. L. (1988). *Mater. Res. Bull.* **23**, 447–452.
Lightfoot, P., Metha, M. A. & Bruce, P. G. (1993). *Science*, **262**, 883–885.
Rabe, G., Roesky, H. W., Stalke, D., Pauer, F. & Sheldrick, G. M. (1991). *J. Organomet. Chem.* **403**, 11–19.
Rietveld, H. M. (1969). *J. Appl. Cryst.* **2**, 65–71.
Seiler, P. & Dunitz, J. D. (1979). *Acta Cryst.* B**35**, 1068–1074.

Seiler, P. & Dunitz, J. D. (1982). *Acta Cryst.* B**38**, 1741–1745.
Stephens, P. W. (1999). *J. Appl. Cryst.* **32**, 281–289.
Takusagawa, F. & Koetzle, T. F. (1979). *Acta Cryst.* B**35**, 1074–1081.
Thompson, P., Cox, D. E. & Hastings, J. B. (1987). *J. Appl. Cryst.* **20**, 79–83.
Visser, J. W. (1969). *J. Appl. Cryst.* **2**, 89–95.
Weiss, E. (1993). *Angew. Chem. Int. Ed. Engl.* **32**, 1501–1523.
Wessel, J., Lork, E. & Mews, R. (1995). *Angew. Chem. Int. Ed. Engl.* **34**, 2376–2378.
Zerger, R. & Stucky, G. (1974). *J. Organomet. Chem.* **80**, 7–17.